Journal of Catalysis **211,** 109–118 (2002)
doi:10.1006/jcat.2002.3696

Nature of Active Sites in the Oxidation of Benzene to Phenol with N_2O over H–ZSM-5 with Low Fe Concentrations

Petr Kubánek, Blanka Wichterlová,[1] and Zdeněk Sobalík

J. Heyrovský Institute of Physical Chemistry, Academy of Sciences of the Czech Republic, Dolejškova 3, CZ-182 23 Prague 8, Czech Republic

Received February 15, 2002; revised May 3, 2002; accepted May 23, 2002

Selective oxidation of benzene with N_2O to phenol was investigated at 350 and 450°C on H–ZSM-5 zeolites of different Si/Al composition, with concentrations of iron ranging from 30 to 2000 ppm, and with gallium (1000 ppm). Zeolites dehydrated at 480°C, dehydroxylated at 720°C, and steamed at temperatures ranging from 500 to 780°C as well as zeolites exchanged by NaCl and treated in NaOH solution were used. IR spectra of OH groups and of adsorbed d_3-acetonitrile on zeolites were employed to determine the concentration of Brønsted and Al-Lewis sites. ESR spectra of Fe(III) ions and IR spectra of perturbed framework T–O–T bonds due to the presence of Fe(II) ions at cationic sites of the reduced zeolites were applied to determine the location of Fe ions in zeolites. The rate of phenol formation correlated with the concentration of Fe in the zeolite but was not affected by the presence of gallium. With all the steamed zeolites the rate of phenol formation increased substantially compared to that of dehydrated zeolites. In contrast, no correlation was found between the concentration of the Brønsted or Al-Lewis sites and the rate of phenol formation. The Fe ions with a complex oxo-structure were found to be the active sites for benzene oxidation with N_2O to phenol. They are reflected in the characteristic ESR signals of Fe(III) at *g* 6.0 and 5.6, and in the IR band at 935 cm^{-1} of perturbed T–O–T framework bonds due to the Fe(II) ions at cationic sites present in the reduced zeolites.

Key Words: **H–ZSM-5; Fe–zeolites; Fe–oxo species; N_2O oxidation of benzene; hydroxylation; phenol.**

INTRODUCTION

Selective insertion of an oxygen atom into hydrocarbons, such as in the conversion of benzene to phenol, represents a challenge with respect to the one-step production of phenol. Widely used technology of the synthesis of phenol from benzene via cumene is a three-step process resulting in the formation of an equimolar amount of acetone, i.e., an excess of acetone. The direct catalytic oxidation of benzene using nitrous oxide on a FeZSM-5-type catalyst, although using an expensive and environmentally harmful oxidant, presently developed by Monsanto Co. and Boreskov Institute of Catalysis (1), might become a new technology.

[1] To whom correspondence should be addressed. E-mail: wichterl@jh-inst.cas.cz.

There are several controversial discussions in the literature concerning the nature and structure of active sites in zeolites for the hydroxylation of benzene to phenol by N_2O. Suzuki *et al.* (2) and Burch and Howitt (3) suggested that the Brønsted acid sites in H–ZSM-5 are active. This was supported by the finding that, after elimination of all Brønsted sites by Na^+ ion exchange, the zeolites were not active. It was suggested that this was due to a radical mechanism, in which protons of the zeolite participate. Panov and co-workers (1, 4–6) suggested that the extraframework iron species in ZSM-5 are the active sites for benzene-to-phenol oxidation with nitrous oxide. Iron–zeolite catalysts exhibit close to 100% selectivity to phenol at about 30% conversion of benzene. However, the structure of iron-based active sites is still a topic of discussion. Panov *et al.* (5, 6) revealed that iron released from the framework of aluminosilicates and ferrisilicates of the ZSM-5 structure at high calcination temperature into extraframework sites results in the formation of Fe-related α-centeres and a dramatic increase in the zeolite hydroxylation activity. Dinuclear Fe species were suggested to be the active sites. These dinuclear Fe species are expected to capture the atomic oxygen, formed by N_2O decomposition, and transfer it into benzene molecule.

Notté (7), too, concluded that the presence of Brønsted acid sites is essential for benzene-to-phenol hydroxylation together with the α-sites, which are primarily linked to the presence of iron. He showed that a decrease in the number of Brønsted sites after steaming a zeolite increased both the concentration of the active α-sites and the phenol yield. After reaching an optimum concentration of Brønsted sites, further reduction of their number was accompanied by a decrease in the zeolite activity. Notté also suggested that Al-Lewis acidity is not sufficient to cause hydroxylation of benzene to phenol.

On the other hand, Zholobenko *et al.* (8) and Kustov *et al.* (9) report that the strong Al-Lewis sites, which are created during high-temperature dehydroxylation (above 700°C) of H–ZSM-5, drive the reaction. They assume that after decomposition of the N_2O molecule, the resulting surface and very reactive oxygen atom remains bound on coordinatively unsaturated aluminium with Lewis acid properties. A single electron pair of N_2O is suggested as participant

0021-9517/02 $35.00

in a donor–acceptor interaction with a Lewis acid center. Selective oxidation of benzene to phenol, involving participation of chemisorbed oxygen species, was reported to take place above 320°C, with maximum activity at 400°C (9). The lower catalytic activity at higher reaction temperatures was ascribed to a decrease in the concentration of surface oxygens due to a recombination reaction leading to molecular oxygen.

A key role of Al-Lewis acidity in benzene oxidation to phenol with N_2O was also proposed by Motz *et al.* (10), who attributed the enhanced activity of hydrothermally treated H–ZSM-5 to the presence of extraframework Al species exhibiting Lewis acidity. By monitoring tetrahedrally, pentahedrally, and octahedrally coordinated Al by ^{27}Al MAS NMR spectra, they found a correlation between the level of framework dealumination, the amount of extraframework aluminium, and hydroxylation activity. Häfele *et al.* (11) observed catalytic activity for H–(Ga)ZSM-5 zeolites in benzene oxidation to phenol similar to that of H–(Al)ZSM-5. The activity was attributed to the presence of extraframework Ga species.

Zeolite activity in benzene oxidation to phenol has been ascribed to the presence of active sites of various nature. To elucidate the nature and structure of the active sites for benzene oxidation to phenol, we monitored the catalytic activity of H–ZSM-5 zeolites of different composition with respect to aluminium, iron, and gallium in dehydrated, dehydroxylated, and steamed zeolites and correlated the concentrations of protonic, Al-Lewis, and Fe sites of various structures with the rate of benzene oxidation to phenol.

EXPERIMENTAL

Zeolites

Na–ZSM-5 (Si/Al = 14.1, 180 ppm Fe), NH_4–ZSM-5 (Si/Al = 12.5, 200 ppm Fe), and H–ZSM-5 (Si/Al = 300, <50 ppm Fe) were provided by the Institute of Oil and Hydrocarbon Gases, Slovakia, and H–ZSM-5 (Si/Al = 37.5, 410 ppm Fe) was provided by the PQ Corp. The size of the zeolite crystals was 0.1 μm for samples with Si/Al = 12.5 and 37.5, and 2 μm for the sample with Si/Al = 14.1. The Na–ZSM-5 zeolite was transferred into the NH_4 form by repeated (3×) ion exchange with a 0.5 M solution of NH_4NO_3 at room temperature (RT). NH_4–ZSM-5 samples with iron concentrations of 30, 50, and 1200 ppm and crystal size of less than 0.1 μm and NH_4–ZSM-5 zeolites with 1000 ppm of Ga were prepared as follows. A solution of Al nitrate (Fluka) in deionized water was added to the mixture of tetraethyl orthosilicate (Fluka) and ethanol (laboratory grade). Fe nitrate (preparations 7 and 8) and Ga nitrate (preparation 9) were added together with the aluminium source (Table 1). The mixtures were stirred for 90 min, and then a solution of tetrapropylammoniumhydroxide in water (20%, Fluka) was added; the resulting mixture was stirred for the next 90 min. The reaction gel was transferred to a teflon-coated autoclave and crystallized under rotary conditions for 72 h at 170°C. After the synthesis the mixtures were centrifuged to separate the solid. The zeolites were thoroughly washed, dried, and calcined in a stream of dry oxygen at 500°C for 6 h to remove the template. The NH_4 forms of the zeolites were prepared by repeated (3×) ion exchange of the calcined material with 0.5 M NH_4NO_3 at RT. XRD analysis indicated that all the samples had a highly crystalline MFI structure. The elemental analysis was done by X-ray fluorescence spectroscopy and inductively coupled plasma emission spectrometry. The chemical composition of the zeolites is given in Table 1.

TABLE 1

Chemical Composition of ZSM-5 Zeolites

Catalyst no.	Si/Al	Fe (ppm)
1	28.0	30
2	19.5	50
3	300	<50
4	14.1	180
5	12.5	200
6	37.0	410
7	28.0	1200
8	28.0	2000
9	28.0	30/1000[a]

[a] Concentration of Fe/Ga.

Selected NH_4–zeolites were treated in a stream of oxygen containing 30% water vapor at temperatures of 500, 600, 700, or 780°C for 3 h. The zeolites are denoted as 1-a, and so forth. Some steamed zeolites were transformed into Na forms by repeated (3×) ion exchange using 0.1 M NaCl at RT. Sample 4-d, steamed at 600°C, was also treated (3×) with 0.1 M NaOH at RT.

All the zeolites (steamed parent forms, and those treated with NaCl and NaOH) were dehydrated at 480°C in an oxygen stream or under vacuum prior to the spectra measurement and the reaction test. Dehydroxylated samples (1-b and 4-h) were prepared by zeolite calcination in an oxygen stream at 720°C for 3 h without exposure to air humidity (*in situ* dehydroxylation) before the catalytic test and measurements of the spectra.

FTIR Spectroscopy

The concentration of Brønsted and Lewis sites in the zeolites was determined by quantitative analysis of FTIR spectra of adsorbed d_3-acetonitrile. Prior to the measurement of the spectra the zeolites were calcined in a stream of oxygen at 480°C and evacuated at RT. The concentration of Fe(II) ions in cationic positions of the evacuated zeolites at 480°C was monitored by FTIR in the "transmission window" region reflecting perturbation of framework T–O–T bonds. Reduction of the zeolites was carried out by evacuation at

480°C. The spectra were recorded on an FTIR spectrometer (Nicolet Magna 550) equipped with a low-temperature MCT-B detector.

The samples in the form of self-supporting wafers, about 5–6 mg · cm^{-2} thick, were placed in a six-position sample holder in a vacuum cell with NaCl windows and connected to a dosing system for d_3-acetonitrile adsorption. Adsorption of d_3-acetonitrile (1.2 kPa, Aldrich) was carried out at RT with subsequent evacuation for 20 min at the same temperature prior to the measurement of FTIR spectra. The spectra were recorded at RT with 2-cm^{-1} resolution by collecting 200 scans for a single spectrum. The spectra intensities were normalized on a sample thickness of 5.5 mg · cm^{-2} using the integrated area of the zeolite skeletal bands from 1750 to 2100 cm^{-1}. IR bands of adsorbed d_3-acetonitrile were deconvoluted into Gaussian profiles according to a procedure described elsewhere (12). A band at 2297 cm^{-1} was ascribed to the interaction of Brønsted sites (both Si–OH–Al and Si–OH–Fe) with the C≡N group of acetonitrile, while the bands at higher frequencies corresponded to the interaction of the C≡N group with Lewis sites of various types (two types of Al-Lewis sites, at 2325 and 2315 cm^{-1}, and an Fe-Lewis site at 2310 cm^{-1}). The following extinction coefficients (12) were used: $\varepsilon OH = 2.05 \pm 0.05$ cm · μmol^{-1} and $\varepsilon L = 3.62 \pm 0.10$ cm · μmol^{-1} (the latter regardless of type of Lewis site).

The spectral component of T–O–T antisymmetric mode due to Fe(II) at cationic sites is represented by a band at 935 cm^{-1} in the transmission window region in the FTIR spectra (see 13, 14).

ESR Spectroscopy

ESR spectra of Fe(III) ions were monitored in the X-band region (≈9.2 GHz) on an ESR spectrometer (ERS-220, Germany). Spectra were recorded at RT in the region of 30–500 mT. Mn(II) ions in a solid matrix were used as an internal standard. Before the measurements of the spectra the samples were pretreated in a stream of dry oxygen at 480°C for 2 h, cooled to RT, and evacuated for 30 min at 10^{-2} Pa, and the samples were then transferred under vacuum to a quartz cell and sealed.

Measurement of the Catalytic Activity

Oxidation of benzene to phenol was carried out in a catalytic flow setup in a fixed-bed through-flow microreactor. The amount of catalyst used was 0.5 g, and the reaction mixture contained 20 vol% N_2O, 20 vol% benzene, and the rest N_2. The individual flow rates were controlled by mass-controlled flow meters. The total flow rate was 60 ml · min^{-1} and the WHSV, based on benzene, was 5 h^{-1}. Benzene was introduced from a thermostated saturator and N_2O from a gas cylinder. Benzene conversion was always lower than 20%. Prior to the reaction the catalyst was activated in a stream of oxygen at a temperature of 480°C for 1.5 h and then in a nitrogen stream at the reaction temperature for 30 min. The reaction was carried out at 350 or 450°C. The chromatographic analysis of the reaction mixture was performed using an online connected gas chromatograph (HP 5890 II series, model G1540A) with an FID detector and a 75-m low-polar DB-VRX fused silica column. The column enabled separation of the following components: benzene, phenol, benzoquinone, and dihydroxyphenols. The concentration of phenol in the reactor outlet was calculated from the calibration based on a known concentration of phenol in the gas stream. The rate of phenol formation (given in mmol · g^{-1} · h^{-1}) was calculated from the concentration of phenol on the reactor outlet.

RESULTS

Protonic and Al-Related Lewis Sites

To determine the role of protonic and Lewis sites in the oxidation of benzene to phenol with N_2O, H–ZSM-5 zeolites with differing compositions of the Si/Al framework in dehydrated, dehydroxylated, and hydrothermally treated forms were used. The investigated zeolites had different trace concentrations of Fe, ranging from 30 to 1200 ppm. The concentration of Brønsted and Lewis sites in these zeolites was determined by the quantitative analysis of IR spectra of the adsorbed d_3-acetonitrile. Figure 1 illustrates the IR spectra of the adsorbed d_3-acetonitrile on selected, variously treated zeolites (Table 2). The intensity of the band

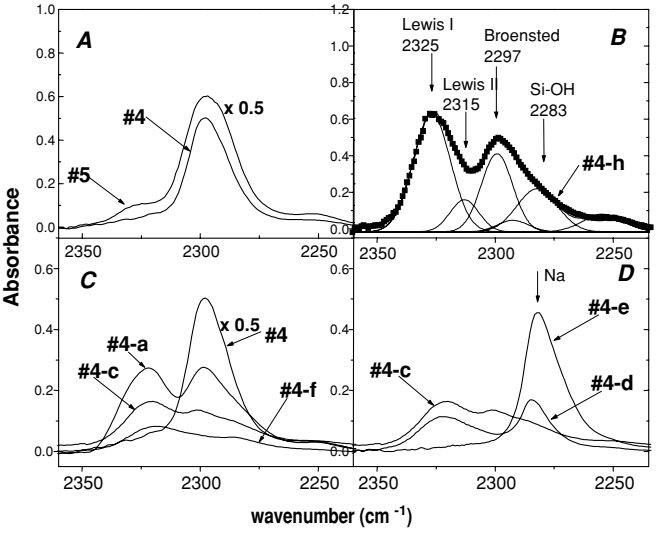

FIG. 1. FTIR spectra of ZSM-5 after d_3-acetonitrile adsorption (10 torr), followed by evacuation at RT in the region of C≡N group vibration. (A) Samples 4 and 5 dehydrated at 480°C. (B) Sample 4-h dehydroxylated at 720°C—illustration of spectra deconvolution. (C) Sample 4 HT at 500°C (4-a), 600°C (4-c), and 700°C (4-f). (D) Sample 4 after HT at 600°C (4-c) and Na^+ ion exchange (4-d) by 0.1 M NaCl and 0.1 M NaOH treatment (4-e).

TABLE 2

Treatment Conditions and Acid Site Concentration of ZSM-5 Zeolites

Catalyst no.	Treatment[a]	Acid site concentration (mmol/g)		Rate of phenol formation (mmol/g · h)	
		Brønsted	Lewis	25 min TOS	125 min TOS
1	C, 480°C	0.37	0.06	0.5	0.5
1-a	HT, 600°C	0.07	0.08	1.4	0.8
1-b	C, 720°C	0.06	0.19	0.5	0.5
2	C, 480°C	0.51	0.07	0.8	0.6
3	C, 480°C	0.03	0.02	0.2	0.1
4-0	Na-form C, 480°C	0.01	0.01	0.3	0.1
4	C, 480°C	0.89	0.08	6.4	3.6
4-a	HT, 500°C	0.18	0.13	8.0	5.7
4-b	HT, 500°C, + IE NaCl	0.06	0.12	8.6	8.0
4-c	HT, 600°C	0.08	0.09	10.2	6.4
4-d	HT, 600°C, + IE NaCl	0.04	0.07	10.5	6.7
4-e	HT, 600°C, + IE NaOH	0.04	0.01	1.5	1.2
4-f	HT, 700°C	0.03	0.05	4.6	3.6
4-g	HT, 700°C, + IE NaCl	0.03	0.03	2.7	2.3
4-h	C, 720°C	0.10	0.48	3.8	1.6
5	C, 480°C	1.05	0.04	6.5	3.6
5-a	HT, 600°C	0.07	0.08	10.0	7.9
5-b	HT, 780°C	0.02	0.02	1.3	0.5
6	C, 480°C	0.26	0.06	7.5	5.2
6-a	HT, 600°C	0.09	0.06	16.1	9.6
7	C, 480°C	0.37	0.06	17.3	10.5
7-a	HT, 600°C	0.07	0.08	29.3	18.1
7-b	HT, 600°C, + IE NaCl	0.05	0.04	28.0	20.0
8	C, 480°C	0.36	0.06	35.0	19.0
8-a	HT, 600°C	0.07	0.08	54.0	38.0
9	C, 480°C	0.36	0.06	0.7	0.5

[a] C, Calcination in a stream of dry oxygen; HT, hydrothermal treatment in a stream of oxygen with 30% H_2O.

at 2297 cm^{-1} was related to the concentration of Brønsted protonic sites. Two types of electron acceptor Lewis sites were distinguished. Type I Lewis sites (of stronger acidity) exhibited a band at 2325 cm^{-1}, while type II Lewis sites (of weaker acidity) were reflected in a band at 2315 cm^{-1} (for details see Ref. (12)). The sum of the concentrations of the Lewis sites (types I and II) was considered in analyzing the effect of the Lewis sites on the catalytic activity of the zeolites. Table 2 lists the concentrations of Brønsted and Lewis sites.

Table 2 clearly shows that the concentration of the protonic sites in dehydrated parent zeolites (Si/Al from 12.5 to 300), in which the number of Brønsted sites highly predominate over that of the Lewis sites (samples 1–9), does not correlate with their hydroxylation activity; e.g., the concentration of the protonic sites in the zeolite with an Si/Al ratio of 12.5 was three times higher that of protonic sites in the zeolite with Si/Al 37. This was not reflected in the higher hydroxylation activity of the former zeolite. The as-synthesized Na–ZSM-5 (sample 4–0) with a very low concentration of Brønsted sites (0.01 mmol · g^{-1}, 180 ppm Fe) was almost inactive, as was the zeolite with Si/Al 300 containing 0.03 mmol · g^{-1} of protonic sites (sample 3, <50 ppm Fe). On the other hand, the steamed NH_4–zeolite exchanged by Na ions (sample 4-d, 180 ppm Fe) exhibited very high activity (see Table 2).

The performance of the dehydrated zeolites 1, 4, and 7 (containing 30, 180, and 1200 ppm Fe, respectively) in time-on-stream (TOS) experiments at 350 and 450°C is shown in Fig. 2. At higher reaction temperature a considerable decrease in activity with TOS was observed; the rate of phenol formation as well as the rate of deactivation were not controlled by the concentration of protonic sites but rather reflected the presence of trace concentrations of iron.

Nearly all the Brønsted sites of zeolites 1 and 4, dehydroxylated at 720°C, were transformed into Lewis sites as follows from a comparison of these concentrations in dehydrated and dehydroxylated zeolites (Table 2). This indicates that under these conditions of zeolite dehydroxylation, the Lewis sites were stabilized at the zeolite framework; one Lewis site was formed from two Brønsted sites. Catalytic tests, carried out at 350 and 450°C over zeolites dehydroxylated at 720°C at *in situ* conditions (without exposure of the zeolite sample to air humidity), did not reveal a significant increase in the rate of phenol formation compared to that of the zeolites calcined at 480°C (Table 2). At the reaction temperature of 350°C the rate of phenol formation on sample 4 was lower for the dehydroxylated zeolite compared to that of the dehydrated zeolite; at a temperature of 450°C H–ZSM-5 containing 30 and 180 ppm of Fe (samples 1 and 4) did not show a significant difference in the activity of dehydrated and dehydroxylated zeolites.

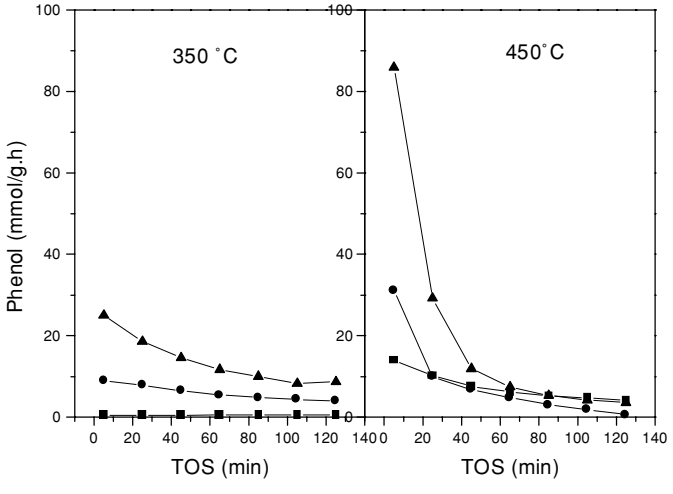

FIG. 2. Dependence of the rate of phenol formation at 350 and 450°C on TOS on H–ZSM-5 dehydrated at 450°C: (■) sample 1 (Si/Al = 28, 30 ppm Fe), (●) sample 4 (Si/Al = 14, 180 ppm Fe), and (▲) sample 7 (Si/Al = 28, 1200 ppm Fe).

At 450°C the deactivation of zeolites in the TOS experiments was higher than at 350°C. Thus the initial reaction rate at this temperature differed for dehydrated and dehydroxylated zeolites (see Fig. 2). Thus, the activities of zeolite catalysts were compared mostly at 350°C. Nevertheless, the results indicate that the strongly acidic Lewis sites are not highly active in the hydroxylation of benzene to phenol.

Hydrothermal treatment of the zeolites (1, 4, 5, 6, 7, and 8) at 500–780°C led to a dramatic decrease in the concentration of Brønsted sites and in the variation of the concentration of Lewis sites. The concentration of Lewis sites in the steamed zeolites did not correspond to a decrease in the concentration of Brønsted sites, such as with the zeolites dehydroxylated under dry conditions without exposure to air. Hydrothermal treatment of zeolites had a dramatic effect on their activity (Table 2, Fig. 3). The rate of formation of phenol over all the steamed NH_4–ZSM-5 zeolites increased and reached a maximum value at a steaming temperature of 600°C. A decrease in catalytic activity was observed above this temperature, and the zeolite hydrothermally treated at 780°C was nearly inactive (sample 5-b, Table 2). This decrease in activity was not caused by a structural collapse of the zeolite, as revealed by XRD, but was due to the expected "clustering" of extraframework Al and Fe species present in zeolites under severe conditions of hydrothermal treatment, as was also indicated by a decrease in the concentration of Al-Lewis sites.

Ion exchange of steamed zeolites in an NaCl solution (samples 4-b vs 4-a and 4-d vs 4-c, respectively) resulted in a decrease in concentration of protonic sites and in only a slight decrease in the concentration of Lewis sites (Table 2). However, the initial rate of phenol formation of "NaCl-exchanged" steamed zeolites did not change significantly, but the deactivation of the catalyst in TOS was suppressed

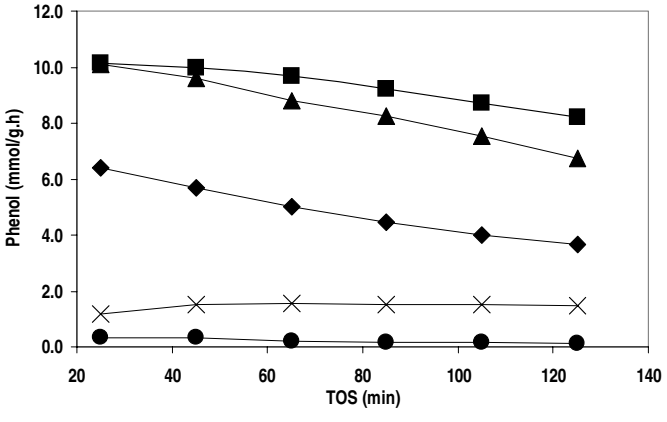

FIG. 3. Dependence of the rate of phenol formation at 350°C on variously treated H–(Al)ZSM-5 (sample 4, Si/Al = 14, 180 ppm Fe): (◆) H–ZSM-5 dehydrated at 480°C, (▲) H–ZSM-5 steamed at 600°C, (■) H–ZSM-5 steamed at 600°C and ion exchanged by 0.1 M NaCl solution, (×) H–ZSM-5 steamed at 600°C and treated with 0.1 M NaOH solution, and (●) original as-synthesized Na–ZSM-5.

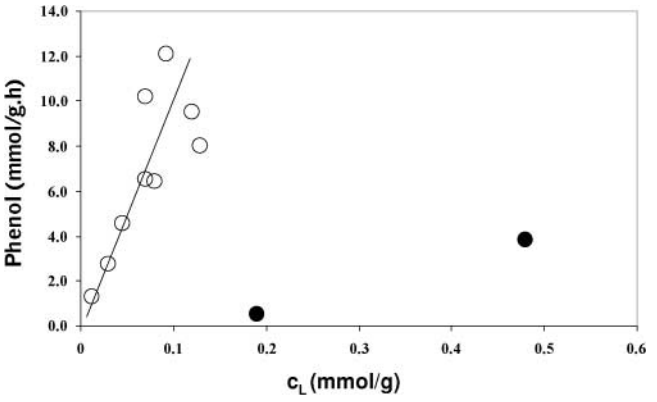

FIG. 4. Dependence of the rate of phenol formation at 350°C on the concentration of Lewis sites on dehydrated, dehydroxylated, and hydrothermally treated zeolites: (●) Lewis sites created by dehydroxylation at 720°C and (○) Lewis sites created by steaming. H–ZSM-5 catalysts derived from samples 1 (30 ppm Fe), 4 (180 ppm Fe), and 5 (200 ppm Fe).

compared to the steamed and dehydrated zeolites (Fig. 3). When the steamed zeolite was washed with NaOH solution (4-e) the concentration of Brønsted sites decreased to the same level as that of the zeolite exchanged with NaCl solution, but almost all the Al-Lewis sites were eliminated. The catalytic activity of such a zeolite dropped dramatically (Table 2, Fig. 3). The remaining concentration of Brønsted sites after treating the zeolite with NaCl and NaOH solutions indicates that some of the protonic sites were probably inaccessible to the exchange. There were no substantial changes in the concentration of Lewis sites after the NaCl treatment, revealing thus a complex structure of Al-Lewis sites.

The dependence of the rate of phenol formation on the concentration of Lewis sites on steamed and dehydroxylated zeolites (Fig. 4) proved that the Lewis sites do not exclusively control the hydroxylation activity of H–ZSM-5 zeolites. Dehydroxylated zeolites with a relatively high concentration of strong Al-Lewis sites sometimes showed lower activity than the steamed zeolites. This indicates that the structure of the Lewis sites was different or that the reaction rate is controlled by the other active sites.

Fe Sites

Dehydrated H–ZSM-5 zeolite (sample 1), with a very low iron content (30 ppm Fe), exhibited almost no catalytic activity in benzene-to-phenol hydroxylation, in contrast to the zeolite containing higher Fe content (Table 2, Fig. 5). Ga ions introduced into the zeolite by adding of trivalent Ga into the crystalization gel (prepared by a synthesis procedure similar to that of samples 1, 7, and 8) have no effect on the catalytic activity (Table 2, cf. samples 1 and 8).

The above results indicate that even trace amounts of the Fe species in zeolites have a decisive effect on the activity of zeolites in the oxidation of benzene to phenol. To

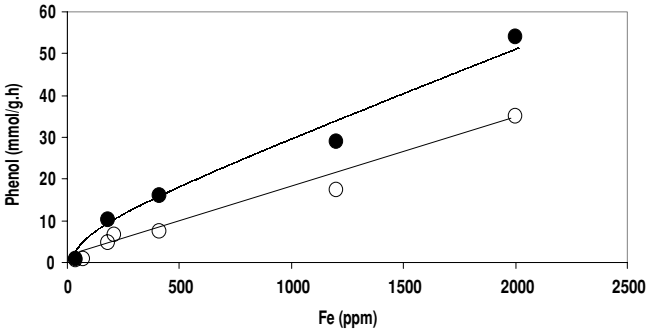

FIG. 5. Dependence of the rate of phenol formation at 350°C on the concentration of Fe in H–ZSM-5: (○) zeolites dehydrated at 480°C, and (●) zeolites steamed at 600°C.

investigate the role of iron in zeolites, particularly of levels present in commercial samples (180–400 ppm Fe for samples 4, 5, and 6), zeolites with very low Fe content (30 and 50 ppm, samples 1 and 2) as well as the sample synthesized with a significantly higher Fe content (7–1200 ppm Fe, 8–2000 ppm Fe) were prepared by the same synthesis procedure. The rate of phenol formation over all these dehydrated H–ZSM-5 zeolites showed nearly linear dependence on the iron content in the zeolites. Zeolite samples 1 and 2 exhibited almost no hydroxylation activity, in contrast to the samples with an iron content exceeding hundreds of parts per million. The strong dependence of the catalytic activity on the iron content of these zeolites is depicted in Fig. 5.

The hydroxylation activity of all the zeolites, including those with a very low Fe concentration, increased significantly with increasing steaming temperature (up to 600°C, Table 2). Figure 5 shows changes in the hydroxylation activity of H–ZSM-5 depending on the concentration of Fe in dehydrated and steamed zeolites at 600°C. The ion exchange of steamed H–ZSM-5 with an NaCl solution (7-b, 1200 ppm Fe) did not result in a change in the catalytic activity, similarly to that of sample 4-d vs 4-c and 4-b vs 4-a, containing a much lower Fe concentration (180 ppm Fe) (Table 2 and Fig. 3).

Figure 6 shows ESR spectra of H–ZSM-5 dehydrated (containing 30–2000 ppm Fe) and after hydrothermal treatment. Three signals of different g values were observed. The signal at g 2.0 (ΔH, 50 mT) is attributed to octahedrally coordinated Fe, while that at g 4.3 (ΔH, 5 mT) is attributed to Fe with tetrahedral coordination (15–17). Signals at g 5.6 and 6.0 (ΔH, 5 mT) were ascribed to isolated Fe(III) cations in highly distorted coordination (18, 19). A broad signal at 2.3 with a width of about 130 mT corresponds to poorly defined iron oxide species exhibiting superparamagnetic behavior.

ESR spectra indicate that most of the iron in the zeolite with 30 ppm Fe (sample 1) was mostly in the form of oxidelike species. We did not detect any other signals or any significant changes in the ESR spectrum of sample 1 after the hydrothermal treatment, because of the very low iron concentration. With concentration of iron increased from 200 to 2000 ppm, the dehydrated zeolites exhibited increasing intensity of the signals at 4.3, 6.0, and 5.6. The different intensity of a broad signal at g 2.3 of the individual zeolites can be due to the different types and concentrations of oxide species formed during the synthesis and postsynthesis treatment of the zeolites. The steaming (up to 600°C) of samples 4, 5, 7, and 8, resulting in a substantial increase in zeolite catalytic activity compared to that of the dehydrated zeolites, led to a considerable increase in the intensity of all the signals, at g 4.3, 5.6, and 6.0. However, the much more severe conditions of the hydrothermal treatment (780°C) of sample 5 (200 ppm Fe) caused diminishing of the signals at g 6.0 and 5.6, while the signal intensity at g 4.3 remained unchanged. Such severe steaming resulted in a substantial decrease in the hydroxylation activity of the zeolite (cf. Table 2).

The ESR results imply the importance of the signals at g 6.0 and 5.6 for the hydroxylation activity of zeolites. Figure 7 depicts the dependence of the rate of phenol formation on the sum of the signal intensities at g 6.0 and 5.6. The rate of phenol formation of the steamed zeolites (full points) correlates to some extent with the intensities of these ESR signals.

In accordance with the other divalent cation-exchanged zeolites (13, 14), the presence of Fe(II) at cationic positions of ZSM-5 zeolites is indicated by a spectral component in the transmission window region represented by a band at

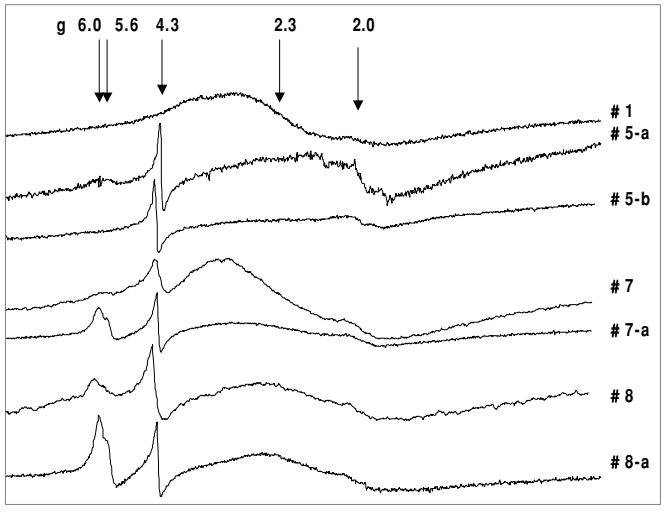

FIG. 6. X-band ESR spectra of H–ZSM-5 with different concentrations of iron and treated under various conditions: (1) 30 ppm Fe, dehydrated at 450°C; (5-a) 200 ppm Fe, HT at 600°C, dehydrated at 480°C; (5-b) 200 ppm Fe, HT at 780°C, dehydrated at 480°C; (7) 1200 ppm Fe, dehydrated at 480°C; (7-a) 1200 ppm Fe, HT at 600°C, dehydrated at 480°C; (8) 2000 ppm Fe, dehydrated at 480°C; and (8-a) 2000 ppm Fe, HT at 600°C, dehydrated at 480°C.

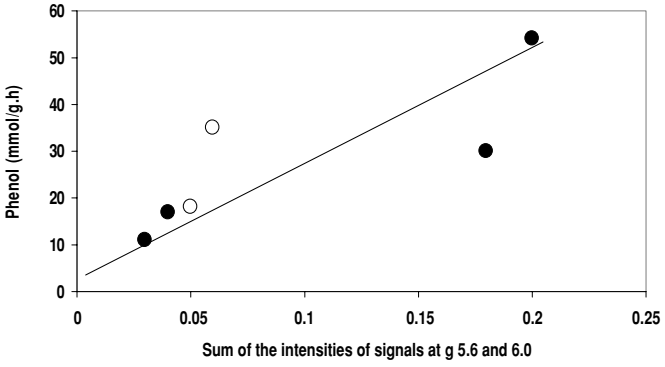

FIG. 7. Dependence of the rate of phenol formation at 350°C (TOS, 25 min) on the intensity of the ESR signals at g 6.0 and 5.6: zeolites (○) dehydrated at 480°C and (●) steamed at 600°C.

about 935 cm^{-1}. This spectral component is assigned to perturbation of an antisymmetric T–O vibration of the zeolite local framework structure due to bonding of the Fe(II) ions.

Figure 8 illustrates IR spectra in the region of skeletal vibrations for samples 1 (30 ppm Fe), 7 (1200 ppm), and 8 (2000 ppm Fe) and for sample 8 after hydrothermal treatment; all were evacuated at 480°C. While the sample with the lowest iron concentration (30 ppm) did not display visible absorption at 935 cm^{-1}, this band was clearly detected with the dehydrated zeolites and increased substantially in intensity for the steamed zeolite. The band represents Fe(II) at the cationic sites (13, 14), formed by the high temperature of the evacuation. The absorption around 900 cm^{-1}, observed with all the zeolites, regardless of iron concentration, is ascribed to defect sites connected with framework aluminium. Although quantitative analysis of the intensity of the band at 935 cm^{-1} is difficult at such low iron concentration, the increase in the intensity of the 935 cm^{-1} band of the Fe at cationic sites indicates a possible relationship to the higher activity of the steamed compared to the dehydrated zeolites.

It is clear that the active Fe sites in zeolites with a low iron content are only a small part of the total content. If this part is estimated to be about 10%, then the turnover frequency (TOF) values, as estimated for sample 8-a , for the Fe active sites might be about 15,000 h^{-1}. This represents very high activity of the active site.

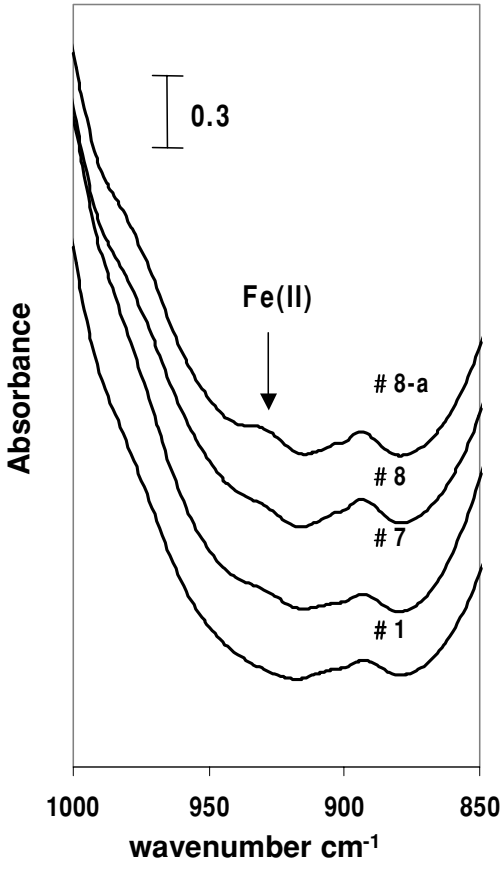

FIG. 8. FTIR spectra in the region of skeletal vibrations for H–ZSM-5 containing Fe(II) ions at cationic positions. Zeolite samples evacuated at 480°C: 1 (30 ppm Fe), 7 (1200 ppm Fe), 8 (2000 ppm Fe), and 8-a (2000 ppm Fe) HT at 600°C.

DISCUSSION

Contribution of Fe Sites to Phenol Formation

Based on the investigations of the concentration of protonic Brønsted sites, Al-related Lewis sites, and Fe sites of various structure and catalytic activity of H–ZSM-5 zeolites with Fe concentrations from 30 to 2000 ppm, in dehydrated, dehydroxylated, and steamed forms, we found that the presence of Fe is decisive for the redox activity of the zeolites. Even Fe concentrations of about 200–400 ppm, as found in commercial samples or in those prepared under standard conditions, result in high activity in the oxidation of benzene with N_2O. Figure 5 shows that regardless of the state of iron, a nearly linear dependence of the rate of phenol formation on the Fe concentration was found with our samples. The location and structure of the Fe sites is important for their redox activity, as revealed by a much higher activity of the samples after steaming. The presence of extraframework Fe species at cationic sites, particularly with steamed and evacuated H–zeolites, was indicated by perturbation of framework T–O–T bonds (IR band at 935 cm^{-1}) due to divalent cation coordination. The development of the active specific Fe structure in variously treated zeolites is also supported by the finding that the activity increases with increasing temperature of steaming to an optimum value, but that more-intensive steaming leads to a decrease in activity. The changes in activity with the severity of steaming were also accompanied by formation of various Fe species as identified by ESR of Fe(III) ions. Under all conditions of steaming a signal at g 4.3 indicated the formation of tetrahedrally coordinated Fe ions. With increasing steaming

temperature, the signal at g 4.3 increased and new signals at g 6.0. and g 5.6, ascribed to distorted T_d-coordinated Fe ions, developed (18), with a maximum intensity for sample 4 steamed at 600°C. More-severe steaming (780°C) resulted in the disappearance of the latter signals and a decrease in activity (Fig. 6 and Table 2), but the signal at g 4.3 retained its intensity. This observation indicates that the signal at g 4.3 represents for the most part T_d-coordinated Fe situated in the extraframework "Al–O" clusters and formed by the removal of aluminium from the framework during steaming, and not from the cations at cationic sites (see for details Ref. (22)). In contrast, the signals at g 6.0 and 5.6 of Fe in distorted T_d coordination were ascribed to Fe in cationic sites. A reasonable correlation between the intensity of these signals and hydroxylation activity (Fig. 7) led us to ascribe the hydroxylation activity to these sites. However, we did not observe a broad signal at low magnetic field at g 20 (Ref. (20)), which might indicate coupled spins.

Based on Moessbauer spectra, Panov *et al.* (1, 5, 6) suggested that the extraframework dinuclear Fe species, formed by high-temperature calcination, and bearing bridging oxygens, are the active sites for benzene hydroxylation. Their conclusion about the complex oxo-structure of the Fe active sites is in agreement with our finding that the active Fe species cannot be exchanged by NaCl, in contrast to their easy removal with the alkaline solution. Simple Na^+ ion exchange of steamed zeolites (samples 4-a or 4-b and 4-c or 4-d) did not result in the removal of the active Fe sites, because the activity of the Na^+-exchanged steamed samples was similar to that of the corresponding steamed H–zeolites. The activity of the former steamed Na–zeolites was even slightly higher at longer TOS; their deactivation was lower compared to the steamed H–zeolites (cf. Fig. 3 and Table 2). The finding that the steamed zeolite treated with NaOH solution (4-e) lost its activity also supports the suggestion that the active species are Fe–oxo ions of complex structure. Washing the zeolites with an alkaline solution removes the extraframework alumina and silica material from zeolites (22), and a substantial change in the state of the iron occurs. These changes are currently being studied. Therefore, all the results imply that the active Fe species are extraframework, probably Fe–oxo species.

These findings also confirm that the as-prepared dehydrated Na–ZSM-5 zeolite did not exhibit hydroxylation activity, in contrast to the NH_4–ZSM-5 zeolite of the same origin calcined under the same conditions (cf. Table 2, samples 4-0 and 4, 180 ppm Fe, rate of phenol formation 0.3 and 6.4 $mmol \cdot g^{-1} \cdot h^{-1}$, respectively). The high activity of the latter zeolite is ascribed to extraframework Fe species rather than to the protonic sites, particularly when the activity of the H–ZSM-5 is compared with that of the dehydrated and steamed zeolite. It is well-known that Na ions (and cations in general, in contrast to protons) at cationic sites stabilize the framework Al and Fe atoms against leaching to the extraframework positions, thus preventing the formation of extraframework Al and Fe species. This is also why Al (or Fe) ions are found in the framework positions in the as-synthesized noncalcined NH_4–zeolites after their calcinations; however, Lewis sites are formed, even at a moderate temperature of about 480°C, indicating some leaching of framework atoms into extraframework positions (cf. Ref. (23)).

Contribution of Protonic Sites to Phenol Formation

Reported results (7, 21) show clear dependence of both the concentration of the α-sites and the hydroxylation activity of H–ZSM-5 zeolites on the concentration of the Brønsted sites. In both of these studies one zeolite sample was used, with 250 ppm Fe (7), or with 900 ppm Fe (21). The changes in the concentration of the Brønsted sites were achieved by high-temperature calcination followed by contact of the samples with moisture in the air (21) or by zeolite steaming (7). One study (7) suggests that the protonic sites, adjacent to the α-Fe centers, are indispensable for the activity. In the other study (21), however, the activity was considered to be related only to the Fe sites, because activity of the calcined samples did not change when the samples were exchanged by Na^+ ions. Pérez-Ramírez *et al.* (24) recently proved the decisive role played exclusively by Fe in ZSM-5 for N_2O decomposition, while Al and Ga were found to be irrelevant. Changing the concentration of the Brønsted sites by zeolite dehydroxylation and especially by steaming also caused a dramatic change in the structure of the Fe site. Accordingly, differences in catalytic activity are mainly due to differences in the structure and concentration of the Fe species but not of the protonic sites. Brønsted sites may have some effect on zeolite activity by hydrocarbon molecules, but they do not contribute to the transformation of an oxygen atom into the benzene molecule.

Contribution of Al Lewis Sites to Phenol Formation

While Panov and co-workers (21) and Kustov and co-workers (8, 9) report that their dehydroxylated H–ZSM-5 samples (containing 900 ppm Fe and 50–500 ppm Fe, respectively) were highly active in benzene oxidation to phenol, we did not observe higher activity for the dehydroxylated (720°C) compared to the dehydrated (480°C) H–ZSM-5 zeolites investigated with samples at two Fe concentrations (30 and 180 ppm) (Table 2, samples 1 vs 1-b and 4 vs 4-h). Panov and co-workers ascribed this activity to extraframework α-Fe sites, in contrast to Kustov and co-workers, who attributed the zeolite oxidation activity to Al-related strongly acidic Lewis sites. The experimental procedure explains the difference in our results compared

to their results. Prior to the activity measurements, the dehydroxylated zeolites were subjected to moist air, while the quantitative analysis of the Brønsted and Lewis sites as well as the catalytic test were performed at *in situ*, i.e. without exposure of the dehydroxylated samples to air; therefore, with our *in situ* dehydroxylated samples, an insignificant number of extraframework species were formed, and strongly acidic Al Lewis sites as well as Fe ions were, for the most part, still bound to the framework. This finding again supports the conclusion that the active sites are Fe–oxo cationic species with an extraframework structure.

Motz *et al.* (10) ascribed the activity of the steamed H–ZSM-5 zeolite (using zeolite samples with 120–600 ppm Fe) to the Al-related Lewis sites, because the concentration of the extraframework Al sites was correlated with the activity of the zeolites. We also observed reasonable correlation of the concentration of Al-Lewis sites of the steamed zeolites with the zeolite activity (Ref. (25) and Fig. 4). However, this correlation is not found when the dehydroxylated zeolites are included in the analysis. Moreover, if the zeolites of various Fe concentrations are taken into the account, then the Al-Lewis sites are certainly not the most active sites (cf. Table 2).

A similar hydroxylation activity of the zeolite with a high content of gallium (1000 ppm Ga and 30 ppm Fe), with Ga situated partly in the framework and at extraframework positions, and the activity of the H–ZSM-5 zeolite shows that also Ga-Lewis sites cannot be considered as highly active centers. Thus, the reported hydroxylation activity of H–(Ga)ZSM-5 (11) may also be related to the trace concentration of Fe. It follows that neither Al- nor Ga-related Lewis sites are the most active sites for benzene hydroxylation with N_2O to phenol.

CONCLUSIONS

This study of a set of variously treated H–ZSM-5 zeolites with differing Si/Al framework compositions (12.5–300) and differing Fe concentrations (30–2000 ppm) provided samples with various concentration levels of Brønsted, Al-Lewis, and Fe species of different structures. It has been shown that apparent correlations of the concentration of the defined sites with the catalyst activity can be found. In general, such apparent relationships may lead to the incorrect identification of the most active site, particularly in cases where the active site is highly active but in low concentration and is simultaneously present with a high concentration of other far less active sites.

The study supports the conclusion of Panovs group that the active sites for the hydroxylation of benzene with N_2O to phenol are extraframework Fe species. These active Fe sites, formed by calcination at high temperatures or steaming of H–zeolites leading to the removal of Fe from the framework, have an Fe–oxo structure; they cannot be exchanged by Na^+ ions, but they changed their state and activity as a result of zeolite treatment with an alkaline solution.

A clear correlation of the concentration of strong acid protonic sites with hydroxylation activity was not found. These sites do not represent the redox active sites but can contribute to the process through activation of the hydrocarbon molecule. The presence of protonic sites in zeolites weakens the framework T–O bonds, thus enabling the transfer of framework Fe atoms to extraframework positions, in contrast to the Na forms of zeolites.

Al- and Ga-related Lewis sites were not found to be the active sites. There was an apparent relationship between their concentration and hydroxylation activity. With the increasing concentration of Al-Lewis sites, due to zeolite calcination or steaming, also the much lower starting concentration of the extraframework Fe sites increases, and the latter is responsible for the increased activity of the zeolite in the oxidation of benzene to phenol.

ACKNOWLEDGMENT

The authors thank the Grant Agency of the Academy of Sciences of the Czech Republic for financial support under Project A4040007.

REFERENCES

1. Panov, G. I., Sobolev, V. I., Dubkov, K. A., and Kharitonov, A. S., *in* "Proceedings, 11th International Congress on Catalysis, Baltimore, 1996" (J. Hightower, W. N. Delgass, E. Iglesia, and A. T. Bell, Eds.), P.O. Elsevier, Amsterdam, 1996; *Stud. Surf. Sci. Catal.* **101**, 493 (1996).
2. Suzuki, E., Nakashiro, K., and Ono, Y., *Chem. Lett.* 953 (1988).
3. Burch, R., and Howitt, C., *Appl. Catal. A* **103**, 135 (1993).
4. Kharitonov, A. S., Sheveleva, G. A., Panov, G. I., Sobolev, V. I., Paukshits, Y. A., and Romannikov, V. N., *Appl. Catal. A* **98**, 33 (1993).
5. Panov, G. I., Sobolev, V. I., and Kharitonov, A. S., *J. Mol. Catal.* **61**, 85 (1990).
6. Panov, G. I., Sheveleva, G. A., Kharitonov, A. S., Romannikov, V. N., and Vostrikova, L. A., *Appl. Catal. A* **82**, 31 (1992).
7. Notté, P., *Top. Catal.* **13**, 387 (2000).
8. Zholobenko, V. L., Senchenya, I. N., Kustov, L. M., and Kazansky, V. B., *Kinet. Catal.* **32**, 151 (1991).
9. Kustov, L. M., Tarasov, A. L., Bogdan, V. I., Tyrlov, A. A., and Fulmer, J. W., *Catal. Today* **61**, 123 (2000).
10. Motz, J. L., Heinichen, H., and Hölderich, W. F., *J. Mol. Catal.* **136**, 175 (1998).
11. Häfele, M., Reitzmann, A., Roppelt, D., and Emig, G., *Appl. Catal. A* **150**, 153 (1997).
12. Wichterlová, B., Tvarůžková, Z., Sobalík, Z., and Sarv, P., *Microporous Mesoporous Mater.* **24**, 223 (1998).
13. El-Malki, El-M., Van Santen, R. A., and Sachtler, W. M. H., *J. Catal.* **196**, 212 (2000).
14. Sobalík, Z., Tvarůžková, Z., and Wichterlová, B., *J. Phys. Chem. B.* **102**, 1077 (1998).

15. Wichterlová, B., and Jírů, P., *React. Kinet. Catal. Lett.* **13**, 197 (1980).
16. Kucherov, A. V., and Slinkin, A. A., *Zeolites* **8**, 110 (1988).
17. Goldfarb, D., Bernardo, M., Strohmaier, K. G., Vaughan, D. E. W., and Thomann, H., *J. Am. Chem. Soc.* **116**, 6344 (1994).
18. Kucherov, A.V., Montreuil, C. N., Kucherova, T. N., and Shelef, M., *Catal. Lett.* **56**, 173 (1998).
19. Volodin, A. M., Sobolev, V. I., and Zhidomirov, G. M., *Kinet. Catal.* **39**, 775 (1998).
20. Ribera, A., Arends, I. W. C. E., de Vries, S., Perez-Ramirez, J., and Sheldon, R. A., *J. Catal.* **195**, 287 (2000).
21. Sobolev, V. I., Dubkov, V. A., Paukhstis, E. A., Pirutko, L. V., Rodkin, M. A., Kharitonov, A. S., and Panov G. I., *Appl. Catal. A* **141**, 185 (1996).
22. Wichterlová, B., Kubelková, L., and Nováková, J., *in* "Proceedings, 5th International Conference on Zeolites, Napoli" (L. V. C. Rees, Ed.), p. 373. Leyden, London, 1980.
23. Bortnovsky, O., Melichar, Z., Sobalík, Z., and Wichterlová, B., *Microporous Mesoporous Mater.* **42**, 97 (2001).
24. Pérez-Ramírez, J., Kapteijn, F., Mul, G., and Moulijn, J. A., *Catal. Commun.* **3**, 19 (2002).
25. Wichterlová, B., Kubánek, P., and Sobalík, Z., *in* "Proceedings, Industrial Applications of Zeolites" (G. F. Froment and P. A. Jacobs, Eds.), p. 149. Brugges, Belgium, 2000.